Small-signal and large-signal performance test of high-speed optoelectronics devices

N. H. Zhu, C. Chen, J. W. Sun, E. Y. B. Pun and P. S. Chung

N. H. Zhu, C Chen, and J. W. Sun are with the State Key Laboratory on Integrated Optoelectronics, Institute of Semiconductors, CAS, P. O. Box 912, Beijing 100083, P.R. China

E. Y. B. Pun and P. S. Chung are with the Department of Electronic Engineering, City University of Hong Kong, 83 Tat Chee Avenue, Kowloon, Hong Kong.

ABSTRACT

This paper presents measurement methods for determining the reflection coefficients and frequency responses of semiconductor laser diodes, photodiodes, and EA modulator chips. A novel method for determining the intrinsic frequency responses of laser diodes is also proposed, and applications of the developed measurement methods are discussed. We demonstrate the compensation of bonding wire on the capacitances of both the submount and the laser diode, and present a method for estimating the potential modulation bandwidth of TO packaging technique. Initial study on removing the effects of test fixture on large-signal performances of optoelectronic devices at high data rate is also given.

Keywords: Scattering parameters, measurement, test fixture, intrinsic response, laser diode, parasitic network.

1. INTRODUCTION

Accurate measurements of both small-signal and large-signal performances of high-speed optoelectronic devices are required for the design, fabrication and packaging of these devices. Usually, the test ports of the test instrument are under either 3.5mm or 2.4mm environment. However, the devices under test normally have different ports, such as microstrip lines, coplanar lines, and so on, thus, test fixtures which can adapt the ports of the instrument and the devices are needed for accurate measurements. Microwave network analyzer has become the key instrument for the measurement of small-signal performances of optoelectronic devices. Calibration of the network analyzer with test fixtures is required in order to remove the errors of the instrument and the test fixtures. The measurement accuracy mainly depends on the calibration methods and the standards used.

In Section II, a simple technique for measuring the reflection coefficients of semiconductor laser diodes, photodiodes, and EA modulator chips is proposed and demonstrated. The impedance of all these optoelectronic chips can be deduced from the directly measured reflection coefficient obtained using a calibrated probe. Also, the

Semiconductor and Organic Optoelectronic Materials and Devices, edited by Chung-En Zah, Yi Luo, Shinji Tsuji, Proceedings of SPIE Vol. 5624 (SPIE, Bellingham, WA, 2005) · 0277-786X/05/$15 · doi: 10.1117/12.579690

packaging parasitics of these devices can be determined accurately.

In Section III, the frequency responses of optoelectronic chips are obtained from the directly measured scattering parameters. In the measurement setup, the test fixture consists of a microwave probe, a submount, and bonding wires. It is well known that both the attenuation and the reflection of the test fixture have strong influences on the directly measured frequency responses. The S-parameters of the probe could be determined using the extended short-open-matched load (SOL) method. The effects of the test fixtures can be completely removed using the proposed technique.

Intrinsic frequency responses of a laser diode are important because they impose the upper limit on the bandwidth of the laser diode, and provide useful information about the active region and values of some critical parameters. Section IV presents a new method for extracting the intrinsic responses of a laser diode from S-parameters measured using a calibrated vector network analyzer.

Section V demonstrates the compensation of the bonding wire on the capacitances of both the submount and the laser diode. It is shown that the small-signal performances of TO packaged photodiode and laser diode modules can be improved by properly choosing the length of the bonding wire.

Section VI presents a simple method for estimating the potential modulation bandwidth of TO packaging techniques. This method is based upon the comparison of the frequency responses of the laser diodes and the TO laser modules. It is shown that our TO packaging techniques used in the experiments can potentially achieve a frequency bandwidth of over 10GHz.

The test fixture has significant effects on the large-signal performances of the high-speed optoelectronic devices. Section VII gives a simple method for removing the effects of the test fixture on large-signal performance test of high-speed optoelectronic devices operating above Gb/s. The correction is based upon the time-domain measurements, the frequency-domain measurements, and the Fast Fourier Transforms.

2. REFLECTION COEFFICIENTS OF OPTOELECTRONIC DEVICE CHIPS

For the measurements of reflection coefficients of optoelectronic chips, an HP 8720D network analyzer is used, and a microwave on-wafer probe with two contacts (from Cascade Microtech Inc., Beaver-ton, OR) is one-port calibrated using its corresponding calibration kit, and the measuring reference plane is located at the tip of the probe, so that the devices with coplanar test ports can be measured accurately. Fig. 1 shows the equivalent circuit of a laser diode mounted on a submount. In order to obtain the intrinsic performances of optoelectronic chips, it is necessary to determine the packaging parasitics first, and then subtract the effects of these parasitics from the measured data. The AlN submount with coplanar electrode pattern was measured, and its conductance and capacitance can be obtained from the measured reflection coefficients [1].

In order to determine the bonding wire impedance, two contact pads on the submount were bonded up with two wires. The bonding wires were identical to those used in the laser chip measurement samples. Repeating the above measuring procedures, one can deduce the admittance of the sample from the measured reflection coefficient of the sample, and obtain the bonding wire impedance by subtracting the admittance of the submount from the admittance of the sample.

The laser diode chip was mounted on an AlN submount, and the bonding wires used to make electrical connection to the laser were similar to the ones characterized previously. The sample was also measured using the

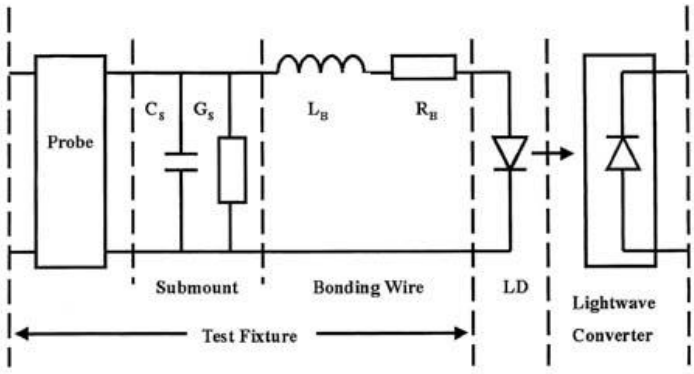

Figure 1: Equivalent circuit of the laser diode mounted on submount.

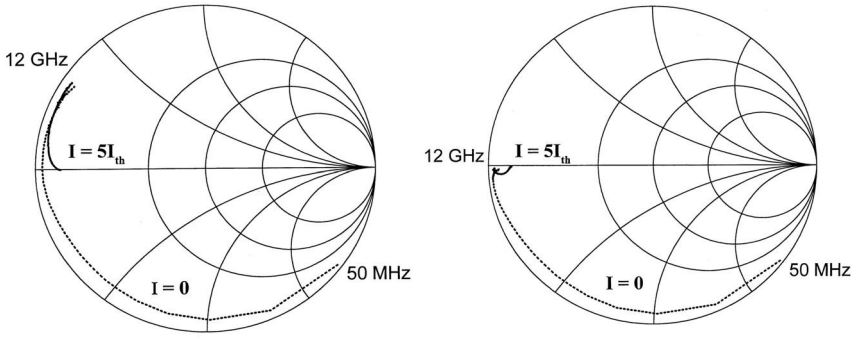

(a) (b)

Figure 2: (a) Directly measured and (b) calculated reflection coefficients of the laser diode

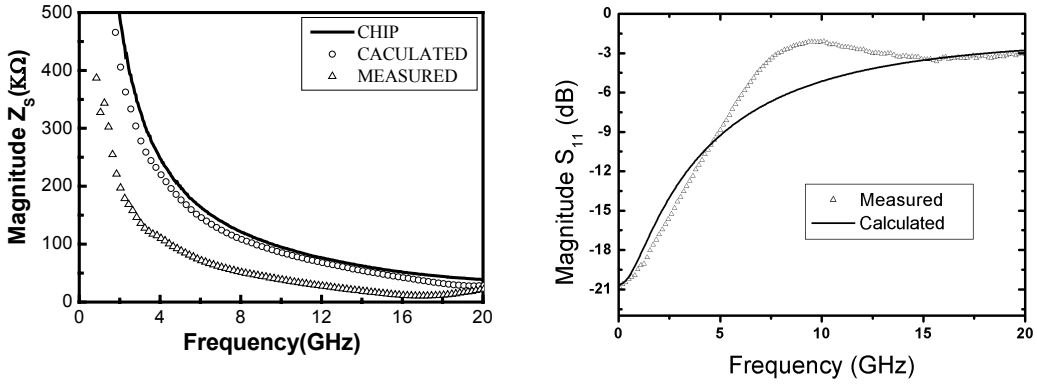

(a) (b)

Figure 3: (a) Measured and calculated impedance of photodiode,
(b) measured and calculated reflection coefficients of the EA modulator.

calibrated probe. The reflection coefficient of the laser diode chip can be calculated from the directly measured reflection coefficient of the laser diode on submount, because all the packaging parasitics have been determined. Fig. 2(a) shows the directly measured reflection coefficient of the laser diode on submount. As can be seen, the

directly measured impedance becomes inductive at frequencies over 100MHz. After removing the submount and bonding wire parasitics, the impedance of the laser diode chip becomes capacitive. The two parallel bonding wires are equivalent to a single 0.2 mm long bonding wire. From Figs. 2(a) and (b), it is clear that such a short bonding wire has strong influence on the impedance.

The proposed method can also be used to measure photodiodes and electro-absorption (EA) modulators integrated with distributed feedback (DFB) lasers. The photodiode is from OptoSpeed and has coplanar electrodes, hence, it can be directly measured using the probe. The measured data can be used to check the accuracy of our method. Fig. 3(a) gives the impedance of the photodiode, and Fig. 3(b) gives the measured and calculated reflection coefficients of the EA modulator. It can be seen that the submount and the bonding wire have some influences on the results, and after removal of their effects, the calculated results are close to the directly measured data.

3. FREQUENCY RESPONSES OF OPTOELECTRONIC DEVICE CHIPS

In the measurements of the frequency response of optoelectronic device chips, an HP 8720D network analyzer was calibrated under the coaxial environment using a full two-port short-open-load-thru (SOLT) calibration technique with the HP85052D 3.5mm calibration standards. In the measurement, the input port of the optoelectronic device chip is coplanar line, and the output port of the detector is coaxial line. Therefore, the test ports of the DUT are under different environments. Unfortunately, the network analyzer can not be calibrated when the two test ports are different, because a known transmission standard is unable to obtain. Thus, the problem to be solved is the characterization of the probe. The extended open-short-load (OSL) method can be used to uniquely determine all scattering parameters of the probe [2]. In our measurement setup, the receiver (HP 11982A) has a flat frequency response and its error factor is negligible [1]. We assume that its frequency response is a constant within the measuring frequency range.

Once all the parameters of the parasitic networks including coplanar probe, submount and bonding wire have been determined, the frequency response of the laser diode can be calculated from the equivalent circuit of the laser diode, and the results are given in Fig. 4.

The proposed method is also used to measure the frequency response of the photodiode and EA modulator integrated with DFB laser. Fig. 5(a) gives the frequency response of a photodiode mounted on the same submount.

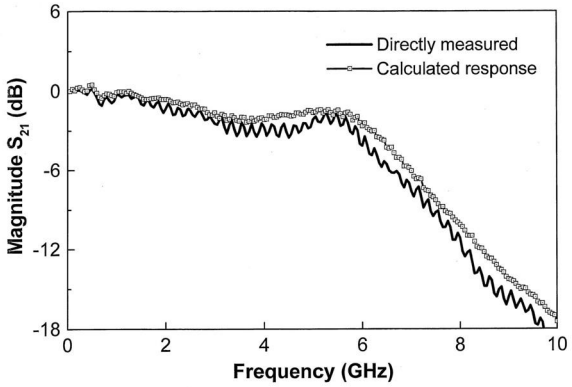

Figure 4: Frequency responses of the laser diode

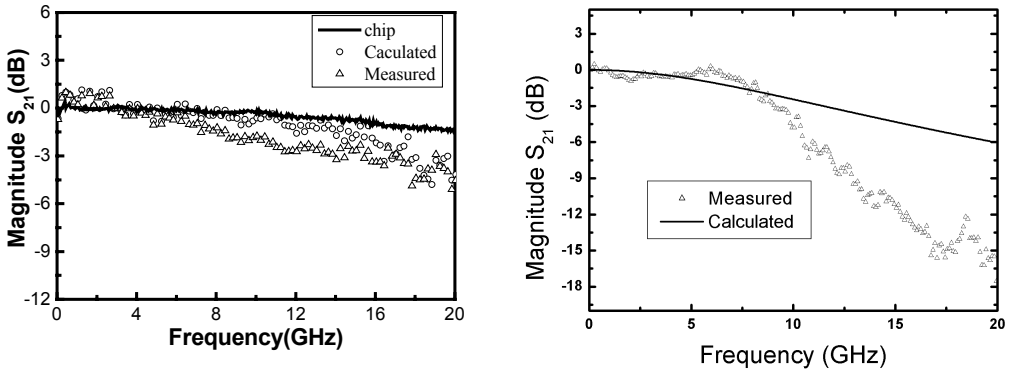

(a) **(b)**

Figure 5: Frequency responses of (a) the photodiode and (b) the EA modulator.

It can be seen that after the effects of the submount and bonding wire are removed, the calculated results agree well with the directly measured data. From Fig. 5(b) one can see that the submount and the bonding wire parasitics have strong influences on the measured results.

4. INTRINSIC FREQUENCY RESPONSE OF LASER DIODE

The intrinsic frequency responses of laser diodes can be obtained using the optical modulation techniques proposed by Su et al. [3], and the frequency response subtraction method [4]. The measurement setup for implementing the first method is constructed using optical fiber components and is shown in Fig. 6. The frequency response subtraction method requires that the parasitic components of the laser diode do not change with the bias current, and the intrinsic response is obtained from the subtraction between the frequency responses of the laser diode at different bias currents. However, the parasitic element values of the equivalent circuit of a laser diode depend on the bias current, as pointed out by Weisser et al. [5]. In the extraction of the parasitic element values, we also found that these values vary with the bias currents. This is the reason why the subtraction method is not as accurate as the optical modulation method.

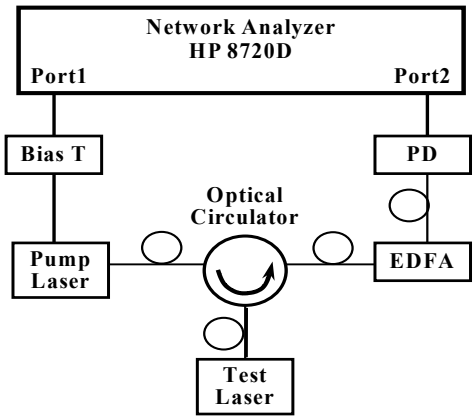

Figure 6: Measurement setup for implementing the optical modulation technique

In the measurements, the laser diode was mounted on one electrode of the submount, and a bonding wire was used to connect the top-contact of the laser diode to another electrode, as shown in Fig.1. The equivalent circuit model of the laser diode mounted on a submount consists of extrinsic parasitic network and intrinsic laser diode, as shown in Fig.7. The parasitics of this structure are usually lumped to be five parasitic elements [3], namely two elements Rc and Cc which are associated with the parasitics of chip, and the other three elements Cp, Rp, Lp are from the submount and the bonding wire. Combining this parasitic network with an ideal laser, a complete model of a laser diode on submount can be established.

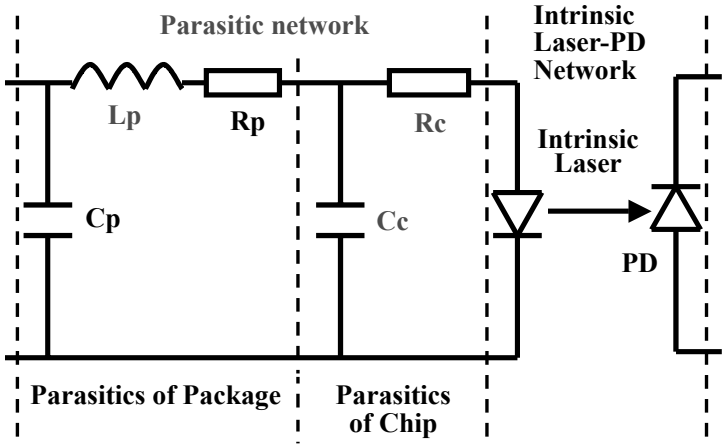

Figure 7: Equivalent circuit model of a laser diode mounted on a submount.

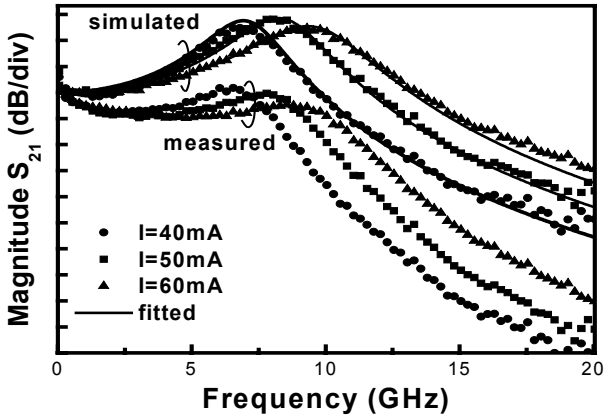

Figure 8: Normalized direct modulation measurements, extracted intrinsic responses and fitting curves to (6)

The S-parameters of the laser diode on submount can be measured using the methods discussed in Sections II and III. From these parameters the element values of the parasitic network can be determined. This is different from the subtraction method [4], since the parameters of the extrinsic parasitic network are functions of the bias current. Finally, the frequency response of the intrinsic laser can be obtained from the equivalent circuit model given in Fig.7 by subtracting the parasitic network from the measured S-parameters of the laser diode. Comparison of the measured data and the intrinsic responses of the laser diode calculated from (7) are shown in Fig. 8.

Fig.9 shows the extract data taken into account the dependence of the damping factor on the square of the relaxation frequency. The results of the optical modulation method [3] and the frequency response subtraction [4] are also included for comparison. There is a good agreement between the results obtained using our method and those directly measured with the optical modulation method, as shown in Fig. 9.

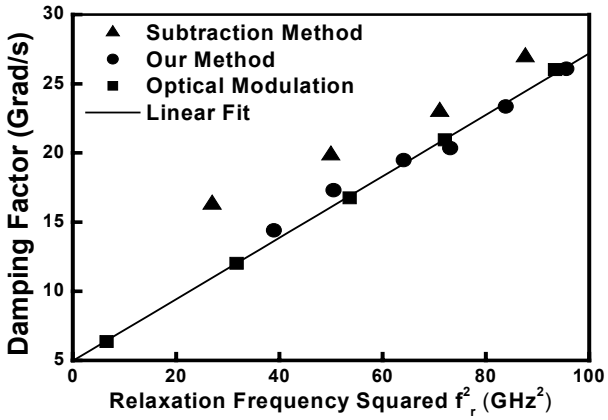

Figure 9: Extracted damping factor versus squared relaxation frequency by three different methods .

From the intercept and slope of the linear fit, an effective carrier recombination time and a K factor can be obtained. Table I summarizes the calculated results extracted using these three methods. It can be seen that our results agree well with those obtained using the optical modulation method.

Table I: Extracted effective carrier recombination time and K factor by three methods

	Subtraction method	Optical modulation	Our method
Effective carrier recombination time	0.09 ns	0.2 ns	0.15 ns
K factor	0.186 ns	0.22 ns	0.20 ns

5. COMPENSATION OF THE BONDING WIRE ON PACKAGING PARASITICS

It has been shown that the cutoff frequency of the chip-to-chip interconnect can be extended by a filter-like compensation [6]. In the electrical connection, the bonding wire and the bonding pads are treated as low-pass filters. This design has been shown to be very successful in the matching of a p-i-n photodiode, and the performances of the device can be improved by a series inductive tuning [7], [8].

In this Section, the compensation of the bonding wire on the capacitances of both the submount and the laser diode is discussed. In the experiment, 1.55μm DFB laser diodes from Opto Speed SA, Mezzovico, Switzerland and 1.31μm FP laser diodes from Archcom Technology Inc., Azusa, USA, were used. The S-parameters of the laser diodes were accurately measured using the methods discussed in Sections II and III. After the measurements, laser

diodes on submounts were used for assembling the TO laser modules. The TO header is SL01.625.018 produced by Schott Glas, Landshut, Germany.

The same measurement setup was used to test the laser modules, and a specially designed test fixture is used instead of the on-wafer probe. The test fixture is a transit from the coaxial to the pins of the TO header. Because there is no corresponding standard for the output test port of the fixture, the test reference plane can only be located at the input test port. Therefore, the effects of the fixture cannot be removed from the measured data. Fig.10(a) gives the comparison of the frequency responses of the 1.55μm DFB laser diode and the TO packaged laser module at different bias currents. Fig. 10(b) shows similar results using 1.31μm FP laser diode.

Usually, the magnitude of the transmission coefficient of the laser diode is larger than that of the TO packaged laser module. As shown in Fig. 10 the response of TO laser module is superior to that of laser diode at some frequencies, especially around 4GHz. It is believed that this is caused by the compensation of the bonding wire on the capacitance of both submount and laser diode. In our case, the submount and laser diode have capacitive

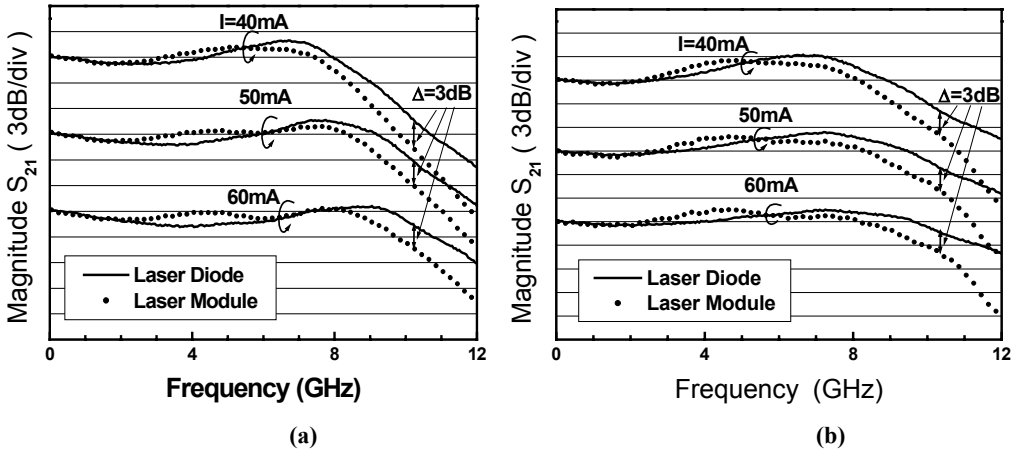

Figure 10: Frequency responses of laser diode and TO laser module at different bias currents.
(a) DFB laser diode from Opto Speed, (b)FP laser diode from Archcom.

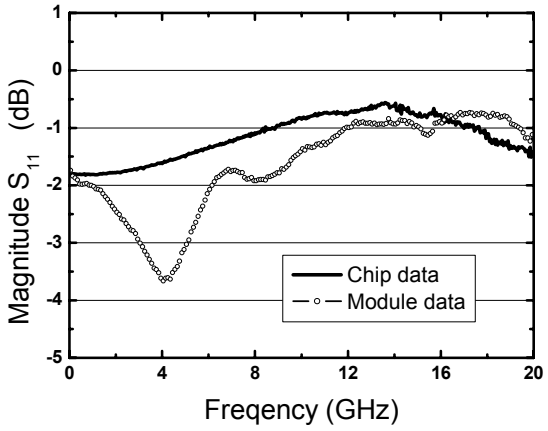

Figure 11: Measured reflection coefficients of the FP laser diode and the TO laser module at a bias current of 40mA.

impedance, and the bonding wire is inductive. The submount, the bonding wire and the bonding pad of the laser diode can be treated as a three-stage low-pass filter which can improve the overall performance of the laser module. From Fig. 11 one can see that the reflection coefficient of the TO laser module has a significant drop at about 4 GHz, compared to that of the laser diode chip. This explains why the transmission coefficient of TO laser module is larger than that of the laser diode at these frequencies.

6. POTENTIAL MODULATION BANDWIDTH OF TO PACKAGING TECHNIQUE

In recent years different kinds of packages, such as TO, butterfly, Mini-DIL, and other specially designed packages have been used for high-speed optoelectronic devices. In these packages, TO package has become a dominant one for high-speed and low-cost laser modules, which have become key components for optical communication systems and Ethernet. TO packaging techniques have drawn increasing attention due to their many attractive advantages, and have been significantly developed and widely used for the TOSA and ROSA. Four years ago, 10Gb/s TO DFB laser modules and TO receiver modules were developed by Ebberg et al. [9], [10]. The directly modulated bandwidth of the laser module with a matching circuit was about 8.2GHz. It is of interest to investigate the upper limit in the frequency bandwidth with this technique. It is also helpful to analyze the effects of packaging and corresponding parasitics on the frequency response of laser modules. The high-frequency performance of the laser modules using the packaging techniques can therefore be improved further.

To the best of our knowledge, packages are not the only limitation on the frequency bandwidth. For a TO laser module, the design of circuit on the submount, and the electrical connections are very critical, in order to achieve a good high-frequency performance. For a butterfly module, the matching circuit and bias network play an even more important role in the packaging of laser modules.

Here, TO laser module is taken as an example to investigate the potential modulation bandwidth achieved with our TO packaging techniques. First, the frequency responses of laser diode chips were measured using the methods discussed in Section II and III. The laser diodes were then carefully packaged in the TO packages in order to achieve high modulation bandwidth, as discussed in Section IV.

An ideal high-speed laser diode should have a constant frequency response within the frequency range concerned. If this ideal laser diode is used, the bandwidth of the packaged laser module can be regarded as the potential bandwidth that can be achieved with this TO packaging technique. In practice, a laser diode always has a finite bandwidth and its reflection coefficient and frequency response vary with frequency. However, the potential bandwidth of the TO packaging techniques can be estimated from the transmission coefficient measurements of both the laser diode chip and the TO packaged laser module. From Fig. 10, one can see that the packaging parasitics strongly affect the frequency response at high frequency. The amount of degradation in the frequency response due to these parasitics reaches 3 dB at about 10.4GHz, and this frequency is regarded as the potential 3-dB bandwidth of the packaging technique used for TO laser modules.

The potential bandwidth should be independent of the bandwidth of the laser diode used in the experiment. From Fig. 10 one can see that the frequency responses of DFB and FP laser diodes are different, and both the laser diode and TO laser module have different 3-dB bandwidths at different bias currents. As expected, the estimated potential 3-dB bandwidth is around 10.4GHz and remains unchanged.

7. EFFECTS OF THE TEST FIXTURE ON LARGE-SIGNAL PERFORMANCE

Eye diagrams and other large-signal characteristics, such as rise time, fall time, jitter, ring, Q factor and extinction ratio, are useful for evaluating devices at high bit rate. Normal measurement system consists of a pattern generator, a sampling oscilloscope, coaxial cables, test fixtures including interface convector, bias network, and the device to be tested. In general, the effects of the pattern generator, the sampling oscilloscope and the test fixtures are also included in the measured results. In order to improve the accuracy of the measurements, the whole system needs to be calibrated. Several approaches to the calibration of large-signal time-domain measurement system have been proposed [11]-[13]. Kompa [13] proposed a relative valid large-signal waveform measurement system, by which the stimulus and reflected waveforms at the DUT reference planes can be determined using a two-channel sampling oscilloscope simultaneously, and the calibration of the measurement system is supported by the vector network analyzer (VNA). Although the system is complicated, the error correction algorithm for the system can evaluate source and load mismatch, tracking, and detractive errors.

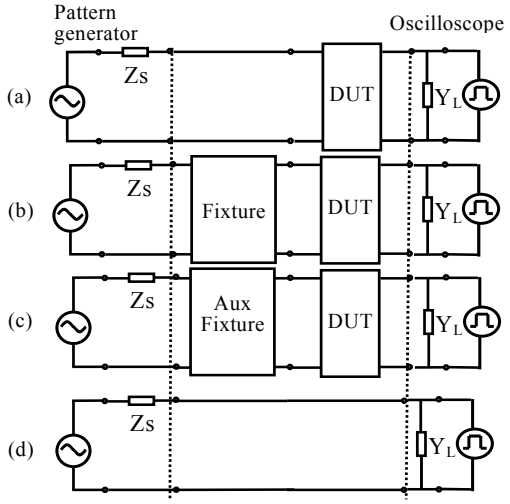

Figure 12: (a) Ideal measurement configuration, (b) Practical measurement configuration with linear fixture, (c) Measurement configuration with linear auxiliary fixture, (d) direct connection.

Here we present a simple correction method based on the frequency-domain measurement of the S-parameter of the test fixture, the time-domain measurement of stimulus and transmitted waveforms, and Fast Fourier Transforms (FFT). Fig. 12 (a) shows an ideal measurement configuration, where ZS is the impedance of the pattern generator and YL is the admittance of the sampling oscilloscope. In most cases, the devices can not be measured directly, and test fixture is needed in the measurement. However, from the hypothetical measurement shown in Fig. 12(a), the relation between the parameters drawing the eye diagram of the DUT and the signal generated by the pattern generator can be obtained. The practical measurement configuration with linear fixture is shown in Fig. 12(b). The scattering parameters of the test fixture can be accurately determined using calibration methods [2]. Since the test fixture is linear, the obtained characteristics can be used to replace the large-signal ones. The measurement shown in Fig. 12(b) can give an independent equation. The measurement shown in Fig.12(c) using another linear auxiliary fixture can also provide another equation. Fig. 12(d) shows the measurement for obtaining the signal generated by

the pattern generator in frequency domain. The transfer function of the DUT can be deduced from the measurements, and the eye diagram can also be drawn based on the waveform calculated from the transfer function.

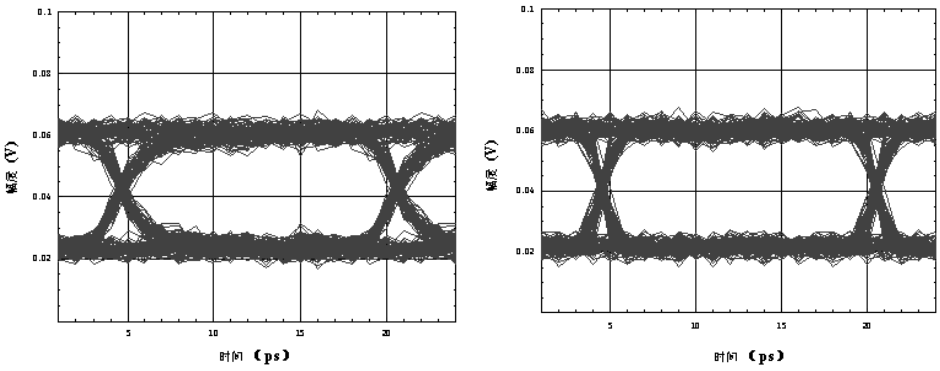

Figure 13: Eye diagrams of the device before and after calibration at a data rate of 10Gb/s

In the measurements, the DUT is an EA modulator integrated with a DFB laser. The RF input port is a GPO connector. In this case, the fixture consists of a GPO-coaxial converter and a bias network. The eye diagrams of the device before and after calibration at a data rate of 10Gb/s are shown in Fig. 13. From the analysis, the rise and fall times reduce from 93.0 ps and 106.0 ps to 34.2 ps and 43.6 ps, respectively, after the calibration. One can see that although the reflection coefficient of the test fixture is very small there are some effects on the measured results.

8. CONCLUSIONS

Methods using microwave network analyzer for determining the reflection coefficients and frequency responses of semiconductor laser diodes, photodiodes, and EA modulator chips have been proposed. Also, a novel method for measuring the intrinsic frequency response of a laser diode is presented, and our experimental results confirm the accuracy of these methods. The applications of our methods to the analyses of the effects of the packaging parasitics are discussed. The errors of the network analyzer and the test fixtures can be completely removed through calibration. However, the calibration of the large-signal time-domain measurement system is difficult.

Our initial study on removing the effects of the test fixtures, pattern generator, and sampling oscilloscope for large-signal performance test appears to be promising. Experimental results show that the accuracy of the large-signal performance test can be improved further using our method.

ACKNOWLEDGMENT

The authors are thankful to Dr. F. Auracher and Mr. S.J.Zhang for several technical discussions. This work is supported in part by the Major State Basic Research Program of China (G2000036601), the National Natural Science Foundation of China (69825109), the National High Technology Development Program, and the CERG (9040804) of the Research Grants Council, Hong Kong.

REFERENCES

1. N.H.Zhu, Y.Liu, E.Y.B.Pun, and P.S.Chung, “Scattering-parameter measurement of laser diodes,” Optical and Quantum Electronics, vol. 34, No.8, pp.747-757, 2002.
2. Z.Y.Chen, Y. L. Wang, Y. Liu, N.H. Zhu, “Two-port calibration of test fixtures with OSL method,” Microwave Opt. Technol. Lett., vol.35, no.4, pp.299-302, 2002.
3. C. B. Su, J. Eom, et al., Characterization of the Dynamics of Semiconductor Lasers Using Optical Modulation, IEEE J. Quantum Electronics, Vol. 28, (1992), 118-127.
4. P.A. Morton, T.Tanbun-Ek, R.A.Logan, et al., Frequency response subtraction for simple measurement of intrinsic laser dynamic properties, IEEE Photon. Technol. Lett., vol. 4, (1992), 133–135.
5. S. Weisser, I. Esquivias, P. J. Tasker, J. D. Ralston, and J. Rosenzweig, Impedance, modulation response, and equivalent circuit of ultra-high-speed In0.35Ga0.65As/GaAs MQW lasers with p-doping, IEEE Photon. Technol. Lett., vol. 6, (1994), 782–785.
6. T.P.Budka, “Wide-bandwidth millimeter-wave bond-wire interconnects,” IEEE Trans. Microwave Theory Tech., vol.49, pp.715-718, 2001.
7. R.Lewén, U.Westergren, R.Schatz, and E.Berland, “Design of inductive p-i-n matching for optical receivers with increased bit-rate operation,” J. Lightwave Technol., vol. LT-19, pp.1956-1963, 2001.
8. K. Yang, A. L. Gutierrez-Aitken, X. Zhang, et al., “Design, modeling, and characterization of monolithically integrated InP-based(1.55μm) high-speed (24Gb/s) p-i-n/HBT front-end photoreceivers,” J. Lightwave Technol., vol.14, pp.1831~1839, 1996.
9. A.Ebberg, F.Auracher, and B.Borchert, “10Gbit/s transmission using directly modulated uncooled MQW ridge waveguide DFB lasers in TO package,” Electron. Lett., vol.36, no.17, 1476-1477, 2000.
10. A.Ebberg, R.Bauknecht, M.Bittner, M.Grumm, and M.Bitter, “High performance optical receiver module for 10Gbit/s application with low cost potential,” Electron. Lett., vol.36, no.8, 741-742, 2000.
11. K. Rush, S. Draving, and J. Kerley, Characterizing high-speed oscilloscopes, IEEE Spectrum 27 (1990), 38-39.
12. M. Sipila, K. Lehtinen, and M.Porra, High-speed frequency periodic time-domain waveform measurement system, IEEE MTT 36 (1988), 1397-1405.
13. G. Kompa and F. Van Raay, Error-corrected large-signal waveform measurement system combing network analyzer and sampling oscilloscope capabilities, IEEE MTT 38 (1990), 358-365.